Effective kinetic energy harvesting via structural instabilities

Ashkan Haji Hosseinloo and Konstantin Turitsyn

Massachusetts Institute of Technology, 77 Massachusetts Ave, Cambridge, USA

ABSTRACT

Vibration energy harvesting has been shown as a promising power source for many small-scale applications mainly because of the considerable reduction in the energy consumption of the electronics, ease of fabrication and implementation of smart materials at small scale, and scalability issues of the conventional batteries. However, conventional energy harvesters are not quite robust to changes in excitation or system parameters, suffer from narrow bandwidth, and are very inefficient at small scale for low frequency harvesting. In addition, they have a low power to volume ratio. To remedy the robustness issues, improve their effectiveness, and increase their power density, we propose to exploit structural instabilities, in particular instabilities in multi-layered composites which are inherently non-resonant. The induced large strains as a result of the structural instability could be exploited to give rise to large strains in an attached piezoelectric layer to generate charge and, hence, energy. The regular high-strain morphological patterns occur throughout the whole composite structure that in turn enable harvesting at a larger volume compared to conventional harvesters; hence, harvesting via structural instabilities can significantly improve the harvested power to volume ratio. In this study, we focus on harvesting from wrinkling type of instabilities.

Keywords: energy harvesting, instability, wrinkling, vibration, piezoelectric

1. INTRODUCTION

Maintenance, replacement, and recharging costs, environmental or health-related complexities, and above all scalability issue of the conventional batteries have convinced researchers to look for other power sources or mechanisms for electronic devices.[1,2] Reduction in power consumption of electronics has made harvesting energy from ambient vibration, a universal and abundant source of energy, a viable alternative to the bulky and costly conventional batteries.[3] However, conventional linear and nonlinear vibratory energy harvesters (VEHs) are not very robust to changes in excitation or system parameters and are not very effective for broadband or low frequency harvesting.

Linear VEHs operating based on linear resonance suffer from narrow bandwidth and are very sensitive to changes in excitation frequency. At the same time, non-stationary and random vibration are in fact more common than harmonic excitation in many practical applications.[4–7] Furthermore, they are extremely inefficient at small scale for low-frequency harvesting as it is either hard to realize the low-frequency resonance at small scale, or the natural frequency of the VEH is bounded from below by an imposed displacement limit.[3] To remedy the issue of narrow bandwidth, purposeful inclusion of nonlinearities, in particular bistability[8–11] has been the focus of many research efforts in the last decade.[12] However, it has been shown that these harvesters work effectively only when the excitation force amplitude is just large enough to trigger interwell oscillations.[13]

Other techniques including up-conversion technique[14–16] and buy-low-sell-high strategy[3,17] have been proposed to improve the low-frequency harvesting efficacy. Although all the above-mentioned methods have improved the harvesting process, they have their own drawbacks including lack of robustness to the system or excitation parameters, being unable to address the two issues of narrow bandwidth and low-frequency harvesting at the same time, or being difficult to implement at the small scale. In addition, the existing harvesting methods often rely on relatively large host structures to realize linear or nonlinear resonance which usually results in low harvested power to volume ratios. For instance, in linear or bistable harvesters, a cantilever beam is often used

Further author information: (Send correspondence to A.H.H.)
A.H.H.: E-mail: ashkanhh@mit.edu, Telephone: +1-(617)-308-9776
K.T.: E-mail: turitsyn@mit.edu , Telephone: +1-(617)-858-1282

Active and Passive Smart Structures and Integrated Systems 2017, edited by
Gyuhae Park, Alper Erturk, Jae-Hung Han, Proc. of SPIE Vol. 10164, 101641G
 · doi: 10.1117/12.2266144

as the host structure and piezoelectric patches for energy transduction are used only close to the clamped end since high strains take place only at the clamped end and at the beam's bottom and top surfaces. This inherent mechanical behaviour consequently results in low power to volume ratios.

In order to overcome the above-discussed issues of the VEHs, one needs to look for a non-resonant mechanism for robust harvesting, that at same time can induce large strains throughout its entire volume as opposed to a small area/volume, so as to improve the harvesting power density. To this end, we propose to exploit instabilities in multi-layered composites or surface instabilities. Unlike classical half-sine buckling of a beam-like structure, instabilities and buckling in composite structures and soft material could take interesting morphological patterns such as wrinkles, folds, and creases[18] that exhibit large strains at regular patterns throughout the entire structure.

Intriguing morphologies and surface patterns in nature at different scales from wrinkles on skins of mammalians, plants and fruits[19–21] to crumpled membranes of blood cells[22] have inspired a big body of research in soft matter instabilities. Recent studies in this field have found applications in other disciplines including soft lithography, metrology, flexible electronics, and biomedical engineering.[18] Here, we extend the application of soft matter instabilities to kinetic energy harvesting.

The induced instability results in large local strains that could be exploited for energy harvesting which is the focus of this paper. The unconventional instabilities are common to the structures that have both stiff and soft components such as a multi-layer composite structure consisting of stiff layers embedded within a soft matrix or a bi-layer structure of a stiff layer sitting on a soft foundation. The large local strain as a result of instability in such structures is the result of two mechanisms: i) when the stiff layers go unstable, they take almost no more load resulting in lower composite stiffness. This consequently leads to large macroscopic strain. ii) the nonlinear geometric pattern of the stiff layer (e.g. sinusoid in wrinkling) locally amplifies the strain. A key advantage of these types of instabilities is that they are independent of the excitation (compressive force) frequency.

In this paper, we focus on wrinkling as the most common instability pattern in composite layers. We derive the state/strain states in a multi-layer composite of a soft matrix containing stiff layers that is subjected to periodic compressive force. We then feed the calculated stresses to piezoelectric patches attached on the troughs and peaks of wrinkling instabilities of the stiff layers and derive the dynamic equation of the electrical domain when the piezoelectric patches are connected to a simple external resistive load. We finally conclude the paper with simulation results and conclusion.

2. MATHEMATICAL MODELING

Surface instabilities are grouped into five main categories: wrinkle, crease, fold, period-double*, and ridge.[23] Based on the phase diagram developed by Wang and Zhao,[23] wrinkling is the most common surface instability if there is no delamination in the layers; hence, we focus on the wrinkling instability in this study. Based on the classic beam theory, a clamped beam buckles under axial compressive force in its first mode (with a mode shape similar to a half sine) before any other modes take place. In fact other modes never take place because they posses larger potential energy than the first mode. However, if the beam is sitting on a softer elastic foundation or embedded in an elastic softer matrix, the beam buckles in higher modes which is usually referred to as wrinkling. The unconventional higher mode buckling occurs simply because the system always seeks a configuration with the lowest potential energy; and above a critical stiffness of the foundation/matrix the higher modes of buckling posses lower potential energy than the classic half-wavelength buckling mode.

When compared to classical buckling, soft matter buckling such as wrinkling has a major advantage of delayed instability. The soft foundation or matrix delays the instability i.e. the structure buckles at a larger critical load. This greatly improves the energy harvesting process by significantly increasing the power inflow to the system. This is because the external force displacement as a result of instability occurs at a larger value of the force; hence, more energy is pumped into the structure. This is in accordance with the buy-low-sell-high strategy where displacement is allowed only at the maximum excitation force magnitude.[3,17]

Figure 1 illustrates schematically how energy is harvested via wrinkling instability. Piezoelectric patches are attached at two sides of the interfacial layers at the peaks and troughs of the wrinkles. Here we assume the

*sometimes period-double or even period-quadruple are categorized under wrinkling, e.g. in[18]

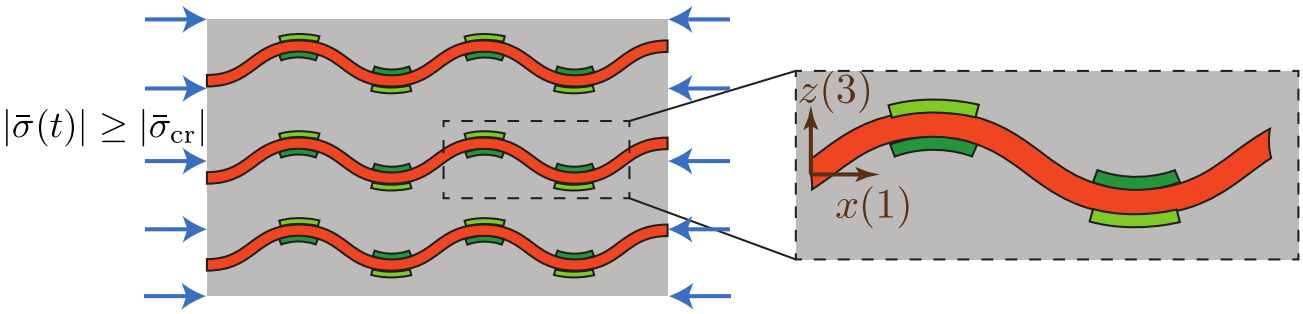

Figure 1. Energy harvesting via wrinkling phenomenon. The figure on the left shows a representative element of a soft matrix containing three stiff interfacial layers/films with piezoelectric patches attached on two sides of the films at the peaks and troughs. The figure illustrates the stiff layers once they have wrinkled. The stiff interfacial layers are straight before wrinkling takes place. The figure on the right depicts larger view of a segment (one wavelength) of the interfacial layer with attached coordinate system where direction x or 1, and z or 3 are aligned with and perpendicular to the interfacial layer, respectively. Wiring and electrical interconnections could be mainly embedded within the soft matrix and the harvesting itself could take place outside the whole structure.

coupling between the piezoelectric patches and the interfacial layer is weak and hence, the piezoelectric effect on the wrinkling phenomenon is negligible; in other words, there is one-way coupling or feedback from the wrinkling layer to the piezoelectric layer. This allows us to study the wrinkling mechanics independent of the piezoelectric layer and then feed the interfacial layer response as the input to the piezoelectric layer. We also assume a plane strain condition. The strains at any point along the interfacial layer are then given by:[24]

$$\begin{aligned} \varepsilon_1(x,z,\bar{\varepsilon}) &= \bar{\varepsilon}_{\rm cr} + \frac{4\pi z}{\lambda(\bar{\varepsilon})}\sqrt{|\bar{\varepsilon}| - |\bar{\varepsilon}_{\rm cr}|}\sin\left(\frac{2\pi x}{\lambda(\bar{\varepsilon})}\right), \\ \varepsilon_3(x,z,\bar{\varepsilon}) &= -\frac{\nu_f}{1-\nu_f}\varepsilon_1(x,z,\bar{\varepsilon}), \\ \varepsilon_{13}(x,z,\bar{\varepsilon}) &\approx 0, \quad \varepsilon_2(x,z,\bar{\varepsilon}) = \varepsilon_{12}(x,z,\bar{\varepsilon}) = \varepsilon_{23}(x,z,\bar{\varepsilon}) = 0. \end{aligned} \tag{1}$$

In Eq.1, $\bar{\varepsilon}_{\rm cr}$ is the critical macroscopic strain at which wrinkling starts, and $\bar{\varepsilon}$ is the applied macroscopic post-buckling strain. $\lambda(\bar{\varepsilon})$ is wavelength of the wrinkle and z is the distance from the neutral axis of the interfacial layer/film in the z or 3 direction. The Poisson ratio of the interfacial layer is denoted by ν_f. Assuming the overall contour length of the interface is preserved, the kinematics enforce that $\lambda(\bar{\varepsilon}) = \lambda_{\rm cr}e^{-|\bar{\varepsilon}|}$ with $\lambda_{\rm cr}$ being the initial wrinkle wavelength.[24] The critical macroscopic strain $\bar{\varepsilon}_{\rm cr}$ and the initial wrinkling wavelength $\lambda_{\rm cr}$ are given by:[25,26]

$$\begin{aligned} \bar{\varepsilon}_{\rm cr} &= -3^{\frac{2}{3}}\left(\tfrac{3-4\nu_m}{(1-\nu_m)^2}\right)^{\frac{-2}{3}}\left(\tfrac{E_f}{E_m}\right)^{-\frac{2}{3}}, \\ \lambda_{\rm cr} &= \pi t\left(\tfrac{1}{3}\right)^{\frac{1}{3}}\left(\tfrac{3-4\nu_m}{(1-\nu_m)^2}\right)^{\frac{1}{3}}\left(\tfrac{E_f}{E_m}\right)^{\frac{1}{3}}, \end{aligned} \tag{2}$$

where, ν_m is the Poisson ratio of the matrix, and E_f and E_m are Young's moduli of the interfacial layer and the matrix, respectively. Thickness of the interfacial layer is designated by t. It should also be noted that for the wrinkling to take place the spacing between interfacial layers cannot be arbitrary. In fact, for a given ratio of the Young's moduli of the soft matrix and stiff layer, spacing between the layers (D) has a lower bound that could be calculated as:[24]

$$\frac{t}{D} < 0.5 - \sqrt{0.25 - 0.24(3-\nu_m)^{\frac{2}{3}}(1+\nu_m)^{-\frac{1}{3}}(\frac{E_f}{E_m})^{-\frac{1}{3}}}. \tag{3}$$

As mentioned earlier, the advantage of exploiting instability for increased local strain is twofold: first, just based on kinematics, the nonlinear instability pattern e.g. Eq. 1 in this study, induces larger local strain than

the macroscopic strain; but more importantly, the macroscopic strain itself is greatly amplified as a result of the instability. This is due to the fact that once the interfacial layer buckles (i.e. wrinkling is initiated), it takes no more load which consequently results in decreased overall stiffness of the composite. The macroscopic strain $\bar{\varepsilon}$ could be mathematically formulated as:[27]

$$\bar{\varepsilon}(t) = \begin{cases} \frac{\bar{\sigma}(t)}{E^i_{\text{comp}}}; & |\bar{\sigma}(t)| < |\bar{\sigma}_{\text{cr}}| \\ \bar{\varepsilon}_{\text{cr}} + \frac{(\bar{\sigma}(t) - \bar{\sigma}_{\text{cr}})}{E^f_{\text{comp}}}; & |\bar{\sigma}(t)| \geq |\bar{\sigma}_{\text{cr}}| \end{cases}, \tag{4}$$

where, $\bar{\sigma}_{\text{cr}} = E^i_{\text{comp}}\bar{\varepsilon}_{\text{cr}}$ is the critical stress at the onset of the wrinkling. E^i_{comp} and E^f_{comp} denote the effective plane-strain Young's modulus of the composite before and after the wrinkling instability, respectively. Effective Young's modulus of the composite before wrinkling could be calculated as $E^i_{\text{comp}} = \eta_m \bar{E}_m + \eta_f \bar{E}_f$ where, η_m and η_f represent volumetric ratios of the matrix and the interfacial layer respectively. Also, $\bar{E}_m = E_m/(1-\nu_m^2)$ and $\bar{E}_f = E_f/(1-\nu_f^2)$ define the plane-strain Young's moduli of the matrix and the interfacial layer respectively. Once the interfacial layers wrinkle, the effective stiffness of the composite drops with a good approximation to $E^f_{\text{comp}} = \eta_m \bar{E}_m$.

Having the full description of the strain states in the interfacial layers which are assumed to be the same as those in the piezoelectric layer, we look into the piezoelectric layer. Polarization direction of the piezo layer is placed along the 3 (z) axis. For plane strain deformation ($\varepsilon_2 = 0$), the strains and the electrical field E_3 along the polarization direction 3(z) satisfy the constitutive relation[28–30] $D_3 = k^s_{33}E_3 + e_{31}\varepsilon_1 + e_{33}\varepsilon_3$, where the electric displacement D_3 is to be found. e_{ij} and k_{ij} are the piezoelectric and the dielectric constants, respectively. In view of Eq.1, ε_3 could be replaced in the piezoelectric constitutive relation, and hence, it could be simplified as:

$$D_3 = k^s_{33}E_3 + \left(e_{31} - \frac{\nu_f}{1-\nu_f}e_{33}\right)\varepsilon_1 \equiv k^s_{33}E_3 + \bar{e}\varepsilon_1. \tag{5}$$

The current running through a piezoelectric layer is calculated by time-differentiating the integral of the electric displacement over the piezo surface as $i = \frac{d}{dt}\int_{A_p} D_3 dA = A_p \dot{D}_3$, where overdot denotes differentiation with respect to time and A_p is the total area of each piezo layer. The last expression is derived assuming that D_3 along the wavelength of the wrinkles is almost constant. This assumption holds for relatively large lengths of piezoelectric layer. The strain gradient along the piezo layers i.e. in x (or 1) direction and hence variability of D_3 in this direction are reflected in Eq.1 in the term: $\sin(\frac{2\pi x}{\lambda(\bar{\varepsilon})})$. This x dependence is absorbed in surface integration when calculating the current i. If the piezo length is not too long relative to the wrinkling wavelength, the sin(.) term could be considered constant over the length and so will be D_3. For simulations in this study, the piezo length is assumed to be 1/6 of the initial wrinkling wavelength i.e. $l_p = 1/6\lambda_{\text{cr}}$. For this case the exact integration yields $i = C\int_{\lambda/6}^{\lambda/3} \sin(2\pi x/\lambda)dx^{\dagger} = C\frac{\lambda}{2\pi}$ while the approximate integration yields $C\frac{\lambda}{6}$. This results in less than 5% discrepancy for a piezo length as large as 1/6 of the wavelength.

We now consider a case where N of the piezo patches are connected in series to an external resistive load characterised by the resistance R. Let's also assume that the electric field E_3 across the thickness of each piezo layer is constant; hence, the voltage across each layer equals $t_p E_3$ with t_p being the piezo layer thickness. Then equating the current running through the resistive load and the piezoelectric layers and substituting D_3 from Eq.5, the governing dynamic equation is derived as:

$$\dot{v} + \left(\frac{Nt_p}{k^s_{33}A_p R}\right)v = -\frac{Nt_p\bar{e}}{k^s_{33}}\dot{\varepsilon}_1. \tag{6}$$

Equation 6 is a first order differential equation that could be solved both analytically and numerically given the input $\dot{\varepsilon}_1$. ε_1 is equal to the macroscopic strain before buckling, but will follow Eq.1 once the buckling takes place. Assuming that the piezo patches are not relatively large in length and are placed at the peaks and troughs, as discussed above, we can approximate $\sin(\frac{2\pi x}{\lambda(\bar{\varepsilon})}) \approx 1$ in Eq.1, and hence the excitation strain rate $\dot{\varepsilon}_1$ in the

[†]C contains all the other constants.

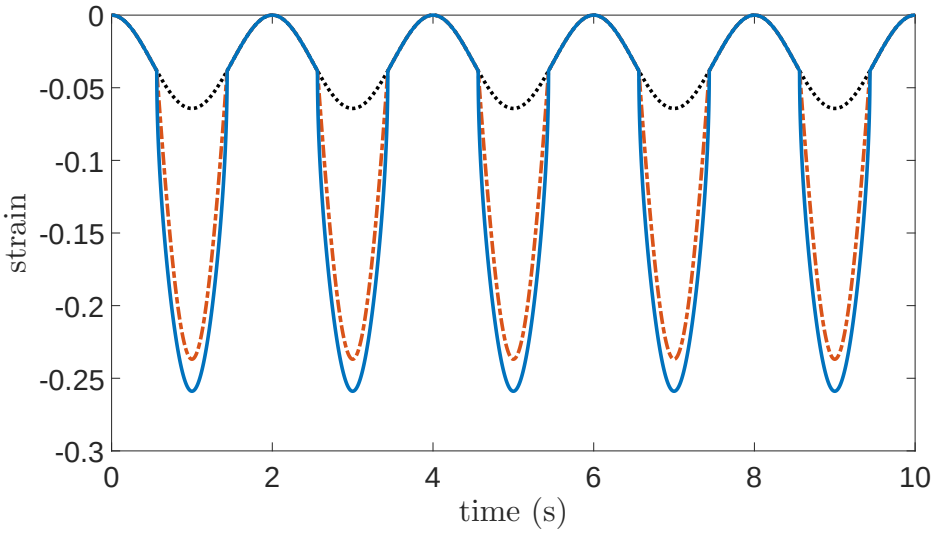

Figure 2. Time history of the induced macroscopic strain $\bar{\varepsilon}(t)$ and the local strain in and along the interfacial layer $\varepsilon_1(t)$. The black dotted line shows the macroscopic and the interfacial layer strain if there was no wrinkling phenomenon. The red dashed-dotted and the blue solid lines represent the macroscopic strain in the composite and the local strain in the interfacial layer in the presence of the wrinkling, respectively.

interfacial and the piezo layers will take the form:

$$\dot{\varepsilon}_1(t) = \begin{cases} \dot{\bar{\varepsilon}}(t); & |\bar{\varepsilon}(t)| < |\bar{\varepsilon}_{\rm cr}| \\ -\frac{4\pi z}{\lambda_{\rm cr}} \left(\frac{|\bar{\varepsilon}(t)|-|\bar{\varepsilon}_{\rm cr}|+0.5}{\sqrt{|\bar{\varepsilon}(t)|-|\bar{\varepsilon}_{\rm cr}|}} \right) \text{sign}(\bar{\varepsilon}(t)) e^{|\bar{\varepsilon}(t)|} \dot{\bar{\varepsilon}}(t); \text{else} \end{cases} \tag{7}$$

Now given the external forcing i.e. $\bar{\sigma}(t)$, Eq. 6 could be solved for the electrical state $v(t)$ in view of the Eqs.4 and 7. Once $v(t)$ is solved, harvested power could be easily calculated. Simulation results are presented and discussed in the next section.

3. NUMERICAL RESULTS AND DISCUSSION

The material properties and the geometric dimensions of the matrix, interfacial layer, and the piezoelectric patches are given in Table 1. b_p in this table denotes the depth of the piezoelectric patches in y (or 2) direction. The length of the piezoelectric patches l_p is set to one sixth of the initial wrinkling wavelength i.e. $l_p = 1/6\lambda_{\rm cr}$. For the parameters in table 1, the critical macroscopic strain $\bar{\varepsilon}_{\rm cr}$, and the initial wavelength $\lambda_{\rm cr}$ are equal to -0.0384 and 0.8027 mm, respectively.

In this study, we consider a slowly-varying sine-squared compressive macroscopic stress $\bar{\sigma}(t) = -\bar{\sigma}_{\rm amp} \sin^2(0.5\omega t)$ with amplitude $\bar{\sigma}_{\rm amp} = 30$ MPa, and frequency $\omega = 2\pi(0.5)$ rad/s. Figure 2 shows the induced macroscopic strain ($\bar{\varepsilon}$) and the local strain along the interfacial layer (ε_1) for $z = -t/2$ in Eq.1 and at the peak of the wrinkle i.e. $\sin(\frac{2\pi x}{\lambda(\bar{\varepsilon})}) = 1$. It could be seen that when the critical strain ($\bar{\varepsilon}_{\rm cr}$=-0.0384) is exceeded, wrinkling takes place and both the magnitude and the rate of the induced strain in the interfacial layer are increased. To have a fair comparison between two cases of harvesting with and without the wrinkling phenomenon, we first optimize the average harvested power with respect to the external load. The average harvested power is defined as the time-average of the dissipated power in the external load: $P_{\rm ave} = \frac{1}{T}\int_0^T \frac{v(t)^2}{R} dt$ for a large value of T. As illustrated in Fig.3, the optimal resistive loads are found to be $2.0 \times 10^{11}\Omega$, and $2.3 \times 10^{11}\Omega$ for the cases with and without the wrinkling, respectively. These optimal loads are used for the rest of the simulations.

As a result of the increased induced strain and its time rate, the external load is excited by a larger current source, and hence, the voltage induced at the external load is increased. Consequently, the energy harvesting is dramatically improved. Figure 4 shows the time histories of the induced voltage and the harvested energy. Based

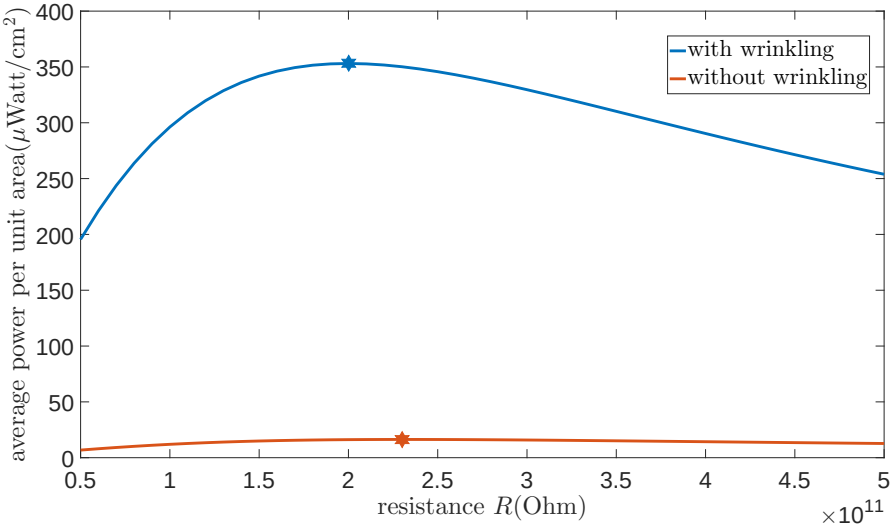

Figure 3. Dependence of the average harvested power on the external resistive load R with and without the wrinkling phenomenon. The optimal load for maximal harvested power is illustrated by hexagrams on each curve. The optimal loads R_{opt} for the cases with and without the wrinkling are $2.0 \times 10^{11}\Omega$, and $2.3 \times 10^{11}\Omega$, respectively.

Parameter	Value
E_m	50 MPa
E_f	5 GPa
ν_m	0.48
ν_f	0.48
t	50 μm
t_p	1 μm
η_f	0.0625
b_p	0.1 mm
e_{31}	-0.3041 C/m^2
e_{33}	-0.4865 C/m^2
k^s_{33}	0.106×10^{-9} C/Vm
N	1

Table 1. Material properties and geometric dimensions of the matrix, interfacial layer, and the piezoelectric patches

on the figure, the induced voltage is increased, and subsequently, the harvested energy is improved by about 20 times. It should be noted that if the whole volume is made of the piezoelectric material (assumed to have large stiffness), a comparable level of energy could be harvested even though no instability takes place and that it compresses uniformly, but at the cost of a much stiffer system which in many applications is not acceptable.

Despite the singularity of $\dot{\varepsilon}_1(t)$ at the start of the instability, Eq.6 is integrable if $e^{\frac{Nt_p}{k^s_{33}A_pR}t}$ is bounded from above. It could also be noticed that if $\frac{Nt_p}{k^s_{33}A_pR} \ll 1$, the induced voltage $v(t)$ is proportional to the induced strain $\varepsilon_1(t)$. For the parameters used for the simulations in this study, $\frac{Nt_p}{k^s_{33}A_pR}$ is not too small (it is about 3.5) so the voltage response is more involved than just being proportional to the strain.

There is another subtle but substantially important reason to the improved harvesting performance in addition to the large induced strains: wrinkling helps the system to passively mimic the BLSH strategy[3] proven by the authors' earlier study to maximize the energy flow into the system. Typical soft matter instabilities occur after a critical applied stress/strain is exceeded. This means the system is not experiencing a large displacement/deformation until a larger value of the excitation force is reached. The larger displacement as a result of the instability, at a large input force simply means larger flow of energy to the system.

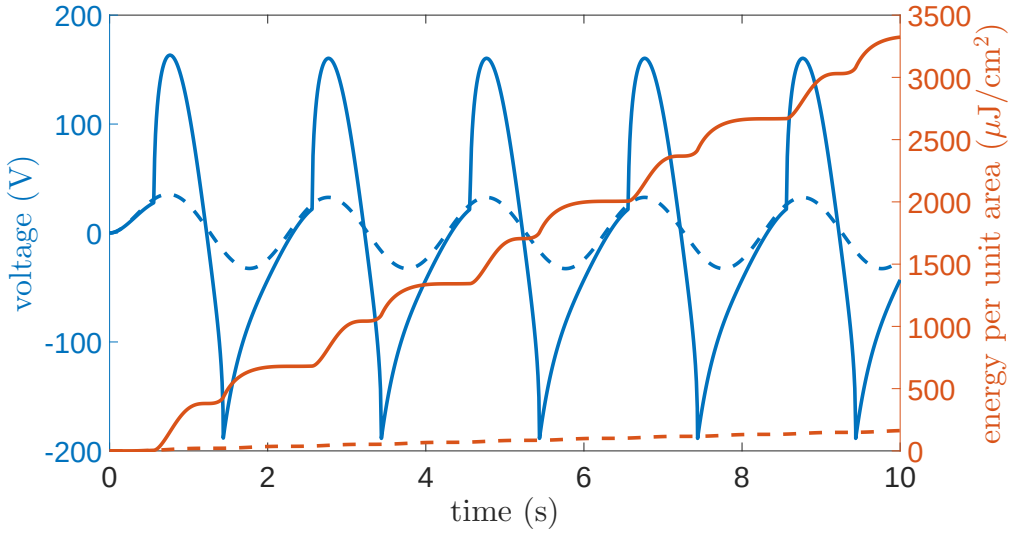

Figure 4. Time history of the induced voltage $v(t)$, and the harvested energy across the external load per unit area of the piezo layer with (solid line) and without (dashed line) the wrinkling phenomenon.

4. CONCLUSIONS

Here we proposed exploiting unconventional structural instabilities for effective kinetic energy harvesting. Structural instabilities allow for large deflections and strains. Instabilities in soft matter and composite structures such as wrinkling, folding, and creasing allow the large local strains take place throughout the entire structure and at regular patterns. Unlike conventional harvesting techniques, this allows to harvest energy from the entire volume of the structure e.g. by attaching piezoelectric patches at large-strain locations throughout the structure. This can significantly improve the power to volume ratio of the harvesting devices. In addition, these structural instabilities are non-resonant that consequently enhances robustness of such harvesters with respect to excitation characteristics. And last but not least, compared to classical buckling, these unconventional instabilities in composite structures occur at a larger external force that will in turn boost the energy flow into the structure.

In this paper, we have particularly focused on wrinkling type of instabilities in composite structures where stiff layers are embedded within a soft matrix. Under large enough compressive force, the stiff layers wrinkle. Energy could be harvested by attaching piezoelectric patches on trough and peaks of the sinusoidal wrinkles where maximum strain is achieved. Here we have assumed one-way coupling between the host structure and the piezoelectric patches i.e. the piezoelectricity does not affect the wrinkling phenomenon. Since we are mainly targeting low-frequency excitation, we assume static stress-strain analysis in the structure which we then feed as the input to the piezoelectric patches. Under low-frequency compressive stress on the structure, we derive the first-order dynamic equation of the electrical state of the system, and consequently calculate the harvested power dissipated in a resistive load connected to the piezoelectric patches. Theoretical and simulation results show that wrinkling could help to increase the harvested power by more than an order of magnitude. We believe the proposed approach opens the way to previously uncharted energy harvesting paradigms, and in view of the recent advances in flexible electronics,[29] introduces a promising method to effectively harvest energy for a wide range of applications.

REFERENCES

[1] Hosseinloo, A. H. and Turitsyn, K., "Optimization of vibratory energy harvesters with stochastic parametric uncertainty: a new perspective," in [*SPIE Smart Structures and Materials+ Nondestructive Evaluation and Health Monitoring*], 97991L–97991L, International Society for Optics and Photonics (2016).

[2] Hosseinloo, A. H. and Turitsyn, K., "Design of vibratory energy harvesters under stochastic parametric uncertainty: a new optimization philosophy," *Smart Materials and Structures* **25**(5), 055023 (2016).

[3] Hosseinloo, A. H. and Turitsyn, K., "Fundamental limits to nonlinear energy harvesting," *Physical Review Applied* **4**(6), 064009 (2015).
[4] Hosseinloo, A. H., Yap, F. F., and Vahdati, N., "Analytical random vibration analysis of boundary-excited thin rectangular plates," *International Journal of Structural Stability and Dynamics* **13**(03), 1250062 (2013).
[5] Hosseinloo, A. H., Yap, F. F., and Chua, E. T., "Random vibration protection of a double-chamber submerged jet impingement cooling system: A continuous model," *Aerospace Science and Technology* **35**, 29–38 (2014).
[6] Hosseinloo, A. H., Tan, S. P., Yap, F. F., and Toh, K. C., "Shock and vibration protection of submerged jet impingement cooling systems: Theory and experiment," *Applied Thermal Engineering* **73**(1), 1076–1086 (2014).
[7] Hosseinloo, A. H., Yap, F. F., and Lim, L. Y., "Design and analysis of shock and random vibration isolation system for a discrete model of submerged jet impingement cooling system," *Journal of Vibration and Control* **21**(3), 468–482 (2015).
[8] Cottone, F., Vocca, H., and Gammaitoni, L., "Nonlinear energy harvesting," *Physical Review Letters* **102**(8), 080601 (2009).
[9] Gammaitoni, L., Neri, I., and Vocca, H., "Nonlinear oscillators for vibration energy harvesting," *Applied Physics Letters* **94**(16), 164102 (2009).
[10] Erturk, A., Hoffmann, J., and Inman, D., "A piezomagnetoelastic structure for broadband vibration energy harvesting," *Applied Physics Letters* **94**(25), 254102 (2009).
[11] Stanton, S. C., McGehee, C. C., and Mann, B. P., "Nonlinear dynamics for broadband energy harvesting: investigation of a bistable piezoelectric inertial generator," *Physica D: Nonlinear Phenomena* **239**(10), 640–653 (2010).
[12] Haji Hosseinloo, A., Slotine, J.-J., and Turitsyn, K., "Robust and adaptive control of coexisting attractors in nonlinear vibratory energy harvesters," *Journal of Vibration and Control* , 1077546316688992 (2017).
[13] Zhao, S. and Erturk, A., "On the stochastic excitation of monostable and bistable electroelastic power generators: relative advantages and tradeoffs in a physical system," *Applied Physics Letters* **102**(10), 103902 (2013).
[14] Kulah, H. and Najafi, K., "Energy scavenging from low-frequency vibrations by using frequency up-conversion for wireless sensor applications," *IEEE Sensors Journal* **8**(3), 261–268 (2008).
[15] Jung, S.-M. and Yun, K.-S., "Energy-harvesting device with mechanical frequency-up conversion mechanism for increased power efficiency and wideband operation," *Applied Physics Letters* **96**(11), 111906 (2010).
[16] Wickenheiser, A. and Garcia, E., "Broadband vibration-based energy harvesting improvement through frequency up-conversion by magnetic excitation," *Smart Materials and Structures* **19**(6), 065020 (2010).
[17] Hosseinloo, A. H. and Turitsyn, K., "Non-resonant energy harvesting via an adaptive bistable potential," *Smart Materials and Structures* **25**(1), 015010 (2015).
[18] Li, B., Cao, Y.-P., Feng, X.-Q., and Gao, H., "Mechanics of morphological instabilities and surface wrinkling in soft materials: a review," *Soft Matter* **8**(21), 5728–5745 (2012).
[19] Cerda, E. and Mahadevan, L., "Geometry and physics of wrinkling," *Physical review letters* **90**(7), 074302 (2003).
[20] Kücken, M. and Newell, A. C., "A model for fingerprint formation," *EPL (Europhysics Letters)* **68**(1), 141 (2004).
[21] Yin, J., Cao, Z., Li, C., Sheinman, I., and Chen, X., "Stress-driven buckling patterns in spheroidal core/shell structures," *Proceedings of the National Academy of Sciences* **105**(49), 19132–19135 (2008).
[22] Wang, L., Castro, C. E., and Boyce, M. C., "Growth strain-induced wrinkled membrane morphology of white blood cells," *Soft Matter* **7**(24), 11319–11324 (2011).
[23] Wang, Q. and Zhao, X., "A three-dimensional phase diagram of growth-induced surface instabilities," *Scientific reports* **5** (2015).
[24] Kaynia, N., *Instability-induced transformation of interfacial layers in composites and its multifunctional applications*, PhD thesis, Massachusetts Institute of Technology (2016).
[25] Allen, H. G., [*Analysis and design of structural sandwich panels.*], Commonwealth and international library. Structures and solid body mechanics division, Oxford ; New York : Pergamon Press, 1969. (1969).

[26] Li, Y., Kaynia, N., Rudykh, S., and Boyce, M. C., "Wrinkling of interfacial layers in stratified composites," *Advanced Engineering Materials* **15**(10), 921–926 (2013).

[27] Haji Hosseinloo, A. and Turitsyn, K., "Energy harvesting via wrinkling instabilities," *Applied Physics Letters* **110**(1), 013901 (2017).

[28] Meitzler, A., Tiersten, H., Warner, A., Berlincourt, D., Couqin, G., and Welsh III, F., "Ieee standard on piezoelectricity," (1988).

[29] Dagdeviren, C., Yang, B. D., Su, Y., Tran, P. L., Joe, P., Anderson, E., Xia, J., Doraiswamy, V., Dehdashti, B., Feng, X., et al., "Conformal piezoelectric energy harvesting and storage from motions of the heart, lung, and diaphragm," *Proceedings of the National Academy of Sciences* **111**(5), 1927–1932 (2014).

[30] Feng, X., Yang, B. D., Liu, Y., Wang, Y., Dagdeviren, C., Liu, Z., Carlson, A., Li, J., Huang, Y., and Rogers, J. A., "Stretchable ferroelectric nanoribbons with wavy configurations on elastomeric substrates," *Acs Nano* **5**(4), 3326–3332 (2011).